Biochemistry

 Volume 14, Number 21 October 21, 1975

Magnesium-Induced Self-Association of Calf Brain Tubulin. I. Stoichiometry†

Ronald P. Frigon‡ and Serge N. Timasheff*

ABSTRACT: The self-association of calf brain tubulin at pH 7.0 in the presence of magnesium ions has been examined by velocity sedimentation. The schlieren patterns were analyzed by methods described by Gilbert and by Cox. The observed process is best described in terms of a rapidly reversible progressive self-association of the tubulin dimer with identical chain elongation equilibrium constants, k, terminated by a ring-closing step, at degree of polymerization $n = 26 \pm 2$, with $k_{26} > k$. The end product of the polymerization reaction has a sedimentation coefficient $s_{20,w}^0 = 42 \pm 2$ S. It is hydrodynamically equivalent to a closed ring structure observed in the electron microscope at identical conditions.

The self-association of tubulin in the presence of magnesium ions has been observed first in sedimentation velocity studies on porcine and calf brain tubulins (Weisenberg et al., 1968; Weisenberg and Timasheff, 1970). From their examination of the behavior of calf brain tubulin, Weisenberg and Timasheff (1970) concluded that, in the presence of optimal concentrations of magnesium ions, a "6S" tubulin species appeared to be in rapid equilibrium with a "30S" species and that the reaction was best thought of in terms of a monomer in rapid equilibrium with a polymer of the same composition. This divalent cation-induced association has not been linked to the self-assembly of microtubules in vitro and may well represent a distinctly alternative reaction. Indeed, the presence of as little as 1×10^{-6} M calcium has been reported to inhibit in vitro microtubule formation (Weisenberg, 1972) although magnesium does not have a similar effect. The repolymerization of tubulin to form microtubules and the specific magnesium ion stimulated self-association of tubulin may, therefore, reflect alternative modes of association of these protein molecules. It seemed, however, that the characterization of the specific interactions involved in either case should be of importance to promoting a better understanding of this complex physiological system. A detailed investigation of the magnesium-induced self-association of purified calf brain tubulin has, therefore, been undertaken, and the results are reported in these papers.

Materials and Methods

Calf brains, for tubulin preparation, were dissected from freshly slaughtered animals, kept on ice, and used within 1–2 hr of slaughter. Distilled, deionized water was used throughout. Guanosine 5′-triphosphate (GTP) was purchased as the Sigma II-S grade, 95–97% pure, and Mann Special Enzyme grade ammonium sulfate was used for tubulin purification. All other chemicals were used as reagent grades without further purification.

Calf brain tubulin was prepared by the method of Weisenberg et al. (1968, 1970), as modified by Lee et al. (1973). Since the stock protein was stored in the presence of 1 M sucrose (Frigon and Lee, 1972), the experimental samples were prepared either by overnight dialysis against the experimental buffer, or by batch equilibration with Sephadex G-25 in PG[1] buffer, followed by elution from a Sephadex G-25 column, preequilibrated with the experimental buffer. The pooled eluate usually contained 60–75% of the initial total protein at a concentration of 15–25 mg/ml.

Tubulin concentrations were determined by diluting aliquots of the samples, either by weight or by volume, into a 40–100-fold quantity of 6 M guanidine hydrochloride and measuring the absorbance of the solutions at 274 nm, using an absorptivity value of 1.15 mg/(mg cm) (Lee et al., 1973).

† Publication 1039 of the Graduate Department of Biochemistry, Brandeis University, Waltham, Massachusetts 02154. *Received May 27, 1975.* Supported by National Institutes of Health Grants GM-14603 and GM-212, National Science Foundation Grant GB-38544X, and a grant from the American Cancer Society, Massachusetts Division.

‡ This work is taken in part from the dissertation submitted by R.P.F. to the Graduate Department of Biochemistry, Brandeis University, in partial fulfillment of the requirements for the degree of Doctor of Philosophy. Present address: Department of Chemistry, University of California, San Diego, La Jolla, California 92037.

[1] Abbreviation used is: PG buffer, pH 7.0, 0.01 M sodium phosphate buffer containing 1×10^{-4} M GTP.

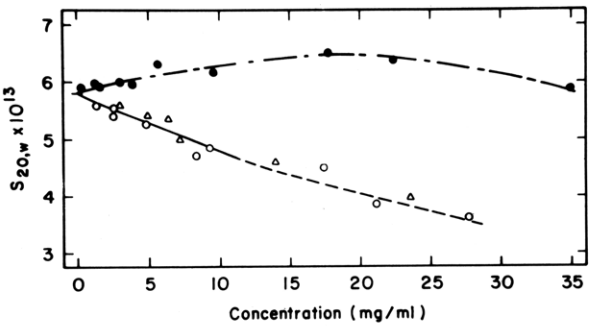

FIGURE 1: Concentration dependence of the sedimentation coefficient of tubulin, as measured at the apex of the schlieren peak. The points ○ and △ were obtained with different protein preparations in PG at pH 7 and 20°. The straight line through the data is a least-squares fit; the dashed portion indicates deviation from linearity. The points ● were obtained in sedimentation experiments in the same buffer with the addition of 0.1 *M* NaCl. The line (- - -) is drawn only to represent the trend in the data.

All sedimentation velocity experiments were performed in a Beckman Model E analytical ultracentrifuge equipped with an electronic speed control and RTIC temperature control. Samples were run in an An-D rotor in 12-mm single or double-sector cells with Kel-F-coated aluminum or aluminum-filled Epon centerpieces and quartz or sapphire windows. Sedimentation profiles were recorded on Kodak metallographic plates. The optical system was aligned by using the method of Richards et al. (1971). Measurements from photographic records were made on a Nikon Model 6C microcomparator. Radial positions of schlieren profiles, x, were recorded either as the peak positions or as the position of the square root of the second moment of the boundary, according to Goldberg (1953):

$$\bar{x}^2 = \int_{x_m}^{x_p} x^2 \left(\frac{\partial n}{\partial x}\right) dx \Big/ \int_{x_m}^{x_p} \left(\frac{\partial n}{\partial x}\right) dx \qquad (1)$$

where $\bar{x}^2$ is the second moment, dn/dx is the gradient of refractive index (schlieren profile), and x_m and x_p are the radial positions of the meniscus and any point in the plateau region, respectively. The measured sedimentation coefficients were corrected to water at 20°, using a value of $\bar{v}$ = 0.736 (Lee and Timasheff, 1974) throughout.

Protein samples for electron microscopy were prepared at 0.1–1.0 mg/ml of tubulin. A drop of each sample was placed on individual carbon-coated Formvar films cast on copper grids and adsorption was allowed to proceed for 1 min. The grids were then blotted and a drop of 1% uranyl acetate was applied to each for 8–16 sec, followed by a rinse with the stain solution and blotting dry. Specimens were examined by using a Phillips Model 300 electron microscope at 80 kV acceleration voltage. The field of view was recorded on 3.25 × 4 in. photographic plates.

Results and Discussion

The Sedimentation Coefficient of Tubulin. When native tubulin, in 0.01 *M* sodium phosphate, 10^{-4} *M* GTP (pH 7.0), 20°, is subjected to sedimentation at 60,000 rpm, a single peak is observed. The corrected sedimentation coefficient, $s_{20,w}$, of the schlieren peak is shown plotted as a function of protein concentration in Figure 1. Fitting of the data below 10 mg/ml of protein to the standard relation (Schachman, 1959)

$$s = s^0(1 - gC) \qquad (2)$$

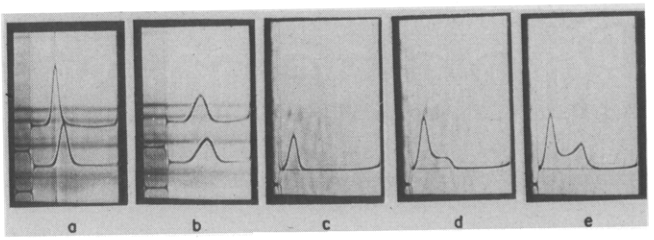

FIGURE 2: Sedimentation patterns of tubulin in PG buffer at pH 7 and 20°. The direction of sedimentation is from left to right; (a and b) 60,000 rpm; (c–e) 48,000 rpm. The protein concentration in each sample of a and b was about 8 mg/ml: (a) 41 min after reaching speed; upper, no magnesium; lower, 0.0027 *M* $MgCl_2$; (b) 38 min after reaching speed; upper, 0.0055 *M* $MgCl_2$; lower, 0.0082 *M* $MgCl_2$; (c–e) 21 min after reaching speed; 0.01 *M* $MgCl_2$; protein concentration, 4.7, 10.4, and 15.5 mg/ml, respectively.

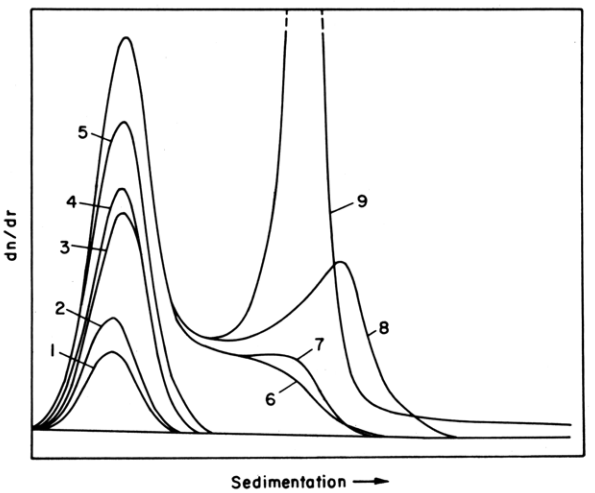

FIGURE 3: Sedimentation velocity profiles of tubulin in PG, pH 7.0, 0.008 *M* $MgCl_2$, 20°, as a function of protein concentration. The superimposed curves are tracings of schlieren profiles taken at a 60° bar angle. The direction of sedimentation is from left to right. The menisci are superimposed on the left margin. The discontinuous profile indicates hypersharpening of the peak. Sedimentation time, 21 min at 48,000 rpm. Protein concentrations (in mg/ml): (1) 1.6; (2) 2.4; (3) 4.9; (4) 7.2; (5) 9.25; (6) 12.2; (7) 16.3; (8) 18.3; (9) 21.6.

resulted in values of $s_{20,w}^0$ = 5.8 S and g = 0.018 ml/mg. At protein concentrations above 10 mg/ml, the data deviate upward, indicating possibly some incipient self-association. The sedimentation coefficient, $s_{20,w}^0$, of tubulin in PG buffer was independent of pH between pH 6.5 and 7.0. In PG at pH 7.0, 20°, in the presence of 0.1 *M* NaCl, however, the sedimentation velocity of the single peak was found to be an increasing function of the protein concentration up to 18 mg/ml followed by a progressive decrease in velocity at higher concentrations, as shown in Figure 1 by the filled circles, indicating incipient association of tubulin in the presence of 0.1 *M* NaCl. Extrapolation to zero protein concentration gave again $s_{20,w}^0$ = 5.8 S.

The Mg^{2+}-Induced Self-Association of Tubulin. Figures 2 and 3 show photos and traced enlargements of typical sedimentation velocity profiles of tubulin as a function of Mg^{2+} ion and protein concentrations. Below 0.01 *M* $MgCl_2$, and at low protein concentrations, increasing the Mg^{2+} concentration results in an increase in the velocity and in the spreading of the single peak, as shown in Figure 2a–c. As the concentrations of Mg^{2+} and protein are increased, a pronounced change in the character of the sedi-

mentation velocity profile, shown in Figure 2d and e and Figure 3, takes place. The sedimentation patterns, which are single peaked at low protein concentration, become bimodal above a given protein concentration. Once bimodality sets in, the area under the slower peak remains constant, all additional protein sedimenting in the rapid peak with a resulting increase in its area.

In Figure 4 are shown the concentration dependences of the sedimentation coefficients of the fast and slow peaks as a function of total protein concentration for different Mg^{2+} concentrations. As seen in Figure 4b, the velocity of the slow peak increases with increasing protein concentration and then levels off at a constant value of close to 9 S as the boundaries become bimodal. The rate of increase in the velocity increases with increasing Mg^{2+} concentration, and the protein concentration at which the boundaries become bimodal decreases with increasing Mg^{2+} concentration. The velocity of the rapid peak, on the other hand, first increases with protein concentration as shown in Figure 4a, then, after reaching a maximum, it slowly decreases with a further increase in protein concentration.

A sedimentation velocity behavior, such as shown in Figures 2–4, is characteristic of a self-associating system in rapid equilibrium relative to the length of the experiment (Gilbert, 1955). Therefore, the velocity of neither the slow nor the fast peak at a finite protein concentration represents the sedimentation of any particular species. In cases, however, where the stoichiometry of the reaction is high, e.g., >10, and the association constant is large, the sedimentation of the observed fast peak may be regarded as closely approximating the sedimentation of the polymeric species (Josephs and Harrington, 1968). The concentration dependence of the fast peak in the decreasing portion of the sedimentation coefficient vs. concentration curve then closely represents the concentration dependence of the polymer and an appropriate extrapolation of this curve back to zero concentration should provide an initial estimate of the apparent sedimentation coefficient of the polymer at infinite dilution.

The sedimentation coefficient of the polymer was obtained, therefore, by plotting the velocity of the fast peak as a function of protein concentration, and extrapolating to zero protein concentration. To meet the criterion of strong association, only hypersharpened fast peaks, which were decreasing in velocity with increasing concentration, were used in this plot. Fitting of eq 2 to the data gives values of g(polymer) = 0.019 ± 0.001 ml/mg and $s_{20,w}{}^0$(polymer) = 41 ± 2 S.

Model of the Self-Association. The character of the sedimentation behavior of tubulin at high $MgCl_2$ concentrations is characteristic of a rapidly reequilibrated self-association reaction of the protein to form a single high molecular weight species with degree of polymerization $n \geq 3$, as described by Gilbert (1955, 1959). Indeed, the fact that the area under the slow peak in the bimodal pattern remains independent of total protein concentration is diagnostic of a classical Gilbert system (Townend et al., 1960). In a simple Gilbert system, however, the velocity of sedimentation of the slow peak should remain constant at a value slightly above that of the velocity of the monomer. In the case of tubulin, however, this velocity is found to increase with increasing protein concentration, as seen in Figure 4. Such an increase in the velocity, as well as the observed spreading of the single slow peak at low $MgCl_2$ and protein concentrations, is characteristic of a progressive self-associating system of the type

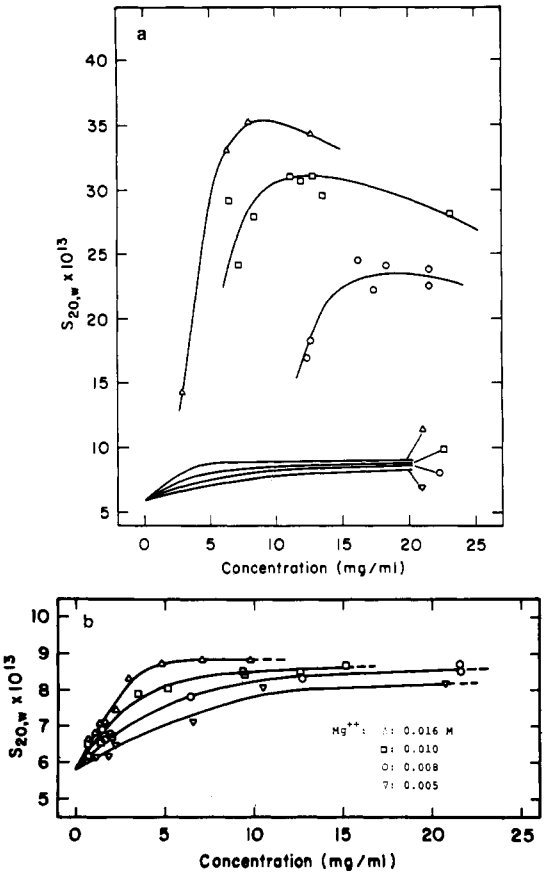

FIGURE 4: Concentration dependence of the sedimentation coefficient of tubulin at various concentrations of $MgCl_2$ in PG, pH 7.0, 20°. (△) 0.016 *M*; (□) 0.010 *M*; (○) 0.008 *M*; (▽) 0.005 *M*. (a) The points are measured sedimentation coefficients of the fast peak, and the curves drawn through the points only indicate the trend. The lower curves represent the sedimentation of the slow peak. In 0.005 *M* $MgCl_2$, no rapid peak formed up to 22 mg/ml of protein. (b) The points are measured sedimentation coefficients of the slow peak, and the curves drawn through the points only indicate the trend.

$$A_1 + A_1 \rightleftarrows A_2;\ k_2 = m_2/m_1{}^2$$
$$A_1 + A_2 \rightleftarrows A_3;\ k_3 = m_3/m_2m_1$$
$$A_1 + A_3 \rightleftarrows A_4;\ k_4 = m_4/m_3m_1$$
$$A_1 + A_{i-1} \rightleftarrows A_i;\ k_i = m_i/m_{i-1}m_1 \qquad (3)$$

where A_i denotes the ith aggregate, the m_i are the molal concentrations of each ith species, and the k_i are the equilibrium constants for successive bond formation between monomer and $(i-1)$-mer. If the k_i in eq 3 are equal ($= k$), the extent of the association is considered as linear indefinite and the reaction is sometimes referred to as isodesmic (Chun et al., 1969, Chun and Kim, 1969, Reisler et al., 1970). For such a system, the sedimentation velocity profile should always be a single forward-skewed peak which increases in velocity with concentration (Holloway and Cox, 1974). An increase in k results in an increase in the velocity at any concentration, as well as in a pronounced increase in spreading of the boundary in the direction of sedimentation (Holloway and Cox, 1974). In an isodesmic self-association system, the weight-average sedimentation coefficient, $\bar{s}$, shows a hyperbolic-like increase with concentration; for a monomer ⇄ polymer type of equilibrium, $\bar{s}$ tends to increase in a sigmoidal fashion (Cox, 1969).

If at any step in the mechanism of eq 3, a particular

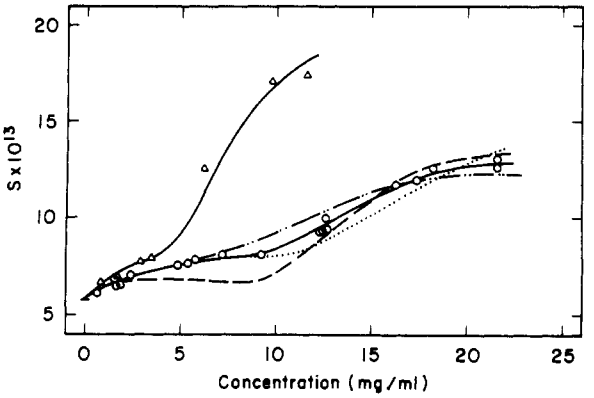

FIGURE 5: Theoretical fitting of the concentration dependence of the weight-average sedimentation coefficient, $\bar{s}_{20,w}$, of tubulin under self-associating conditions in the presence of Mg^{2+}. (○) I, 0.008 *M* $MgCl_2$; (△) II, 0.016 *M* $MgCl_2$. The lines are least-squares fits to the data according to the models described in Table I: (—) I-1 and II-1; (– –) I-2; (– · · –) I-3; (· · ·) I-4.

value of k_i ($i = n$) is considerably larger than k_2, the formation of the *n*th aggregate becomes greatly favored and the polymerization reaction may be terminated by forming the *n*th species. When $k_n \gg k_2$, the self-association behaves essentially as a monomer ⇄ polymer equilibrium (Gilbert, 1959).

From these considerations, the behavior of tubulin during sedimentation at the varied $MgCl_2$ and protein concentrations indicates that this protein undergoes a rapidly reversible self-association reaction which appears to be principally of a monomer ⇄ polymer type, but with a significant amount of intermediate-sized species present in the equilibrium state.

In the quantitative analysis of the data, the two fundamental observations, that at low Mg^{2+} and low protein concentrations, tubulin undergoes what is best described as an indefinite self-association, and that under optimal conditions, a reversible high molecular weight polymer of tubulin is formed, have been expressed as two basic assumptions. The first assumption is that the free energies of formation of bonds between successive aggregates and monomeric units (the tubulin dimer, in this case)[2] are identical and equal to $-RT \ln k$, where $k = k_2 = k_3 = \ldots = k_i = \ldots = k_{n-1}$, as shown in eq 3. The second assumption is that the final step in the self-association is favored, i.e., $k_n > k$.

By expressing the concentration of species *i*, C_i, in units of mg/ml, the intrinsic association constant, *k*, becomes

$$k = K_2 M_1/2$$

$$K_2 = \frac{C_2}{C_1^2}$$

$$K_1 \equiv 1 \qquad (4)$$

where K_2 is the dimerization constant in units of ml/mg and M_1 is the molecular weight of the monomeric unit of the self-association. The equilibrium constants, K_i ($i > 2$), between any *i*-mer and the monomer can each be expressed in terms of K_2 as follows:

$$K_i = i(K_2/2)^{i-1} \qquad (5)$$

[2] It should be emphasized, at the risk of introducing minor confusion, that in the analysis of the data, the tubulin dimer, molecular weight 110,000, will be referred to as the "monomer" of the self-association reaction, unless indicated otherwise.

Table I: Least-Squares Fitting of Weight-Average Sedimentation Velocity Data.

Set	K_2[a]	*n*	s_n^0	g_n	K_n[a]	SSR[b]	σ[c]
I-1	0.2237	26	42	0.019	5.54×10^{-16}	0.68	0.18
I-2	0.3396[d]	26	42	0.019	2.26×10^{-17}	8.33	0.64
I-3	0.2237	13	42	0.019	4.17×10^{-8}	5.91	0.54
I-4	0.2237	26	38	0.019	1.86×10^{-16}	4.09	0.45
I-5	0.2000	26	42	0.019	1.16×10^{-16}	0.84	0.21
I-6	0.2500	26	42	0.019	2.70×10^{-16}	1.07	0.23
II-1	0.3319	26	42	0.019	4.24×10^{-10}	3.26	0.64

[a] Solute concentration expressed in units of mg/ml. [b] The sum of the squares of residuals. [c] Standard root-mean-square deviation. [d] Calculated for a monomer ⇌ dimer ⇌ polymer equilibrium.

The favored formation of a polymer at the *n*th step, which terminates the reaction, can be described by

$$K_n = n(K_2/2)^{n-1}\gamma \qquad (6)$$

The quantity $-RT \ln \gamma$ represents the favorable additional free energy of formation of the polymer (Gilbert, 1955, 1959).

In considering the sedimentation of a reacting system of *n* species in rapid dynamic equilibrium, the rate of movement of the sedimenting reaction boundary is accurately described by the velocity of the square root of the second moment of this boundary. This corresponds to the weight-average sedimentation coefficient, $\bar{s}$ (Schachman, 1959)

$$\bar{s} = \sum_i s_i C_i \Big/ \sum C_i \qquad (7)$$

where s_i is the sedimentation coefficient of the *i*th aggregate. The total weight concentration of protein, *C*, is

$$C = \sum C_i = \sum K_i C_1^i \qquad (8)$$

If each sedimentation coefficient, s_i, is expressed as a function of the total protein concentration, *C*, according to eq 2, then

$$\bar{s} = \sum_i s_i^0 (1 - g_i C) K_i C_1^i \Big/ \sum_i K_i C_1^i \qquad (9)$$

where C_1 is the monomer concentration.

The function $\bar{s}(C, s_i^0, g_i, K_i)$ described by eq 9 was fitted to the experimental weight-average sedimentation coefficients, $\bar{s}_{obsd}$, obtained as a function of *C*, by means of a nonlinear least-squares method (Magar, 1973). The procedure requires good initial estimates of the parameters of the function, s_i^0, g_i, and K_i, and refined values for the parameters are obtained by a reiteration scheme which employs the standard root-mean-square deviation, σ, of the observed data from the calculated curve as a criterion of convergence, where

$$\sigma = \frac{1}{n}\left[\sum_{j=1}^{n} (\bar{s} - \bar{s}_{obsd})_j^2\right]^{1/2} \qquad (10)$$

The method works best when a minimum number of parameters are defined by the function to be fitted (Magar, 1973), and eq 9 was found to admit several simplifications. First, for estimated values of K_2 and K_n, the K_i ($2 < i < n$) were calculated by using eq 5 and the value of C_1 was then obtained as the positive real root of eq 8. In doing the calculation, the monomer values used were: $s_1^0 = 5.8$ S; $g_1 = 0.018$ ml/mg. Since experimental values are not readily measurable for s_i^0 and g_i ($2 \leq i < n$), it was assumed that

the coefficients g_i are identical and equal to $g_1 = 0.018$ ml/mg, and that the s_i^0 are simple functions of $s_1^0 = 5.8$ S:

$$s_i^0 = s_1^0(i)^{2/3} \quad (11)$$

This relationship assumes spherical symmetry for all species (Cann, 1970; Nichol et al., 1964). This last assumption is evidently not strictly true, but any speculation on the nature of the changes in frictional properties of intermediate species (Gilbert, 1963; Holloway and Cox, 1974) would only serve to complicate the model without gaining any additional information. The experimental values of $g_n = 0.019$ ml/mg and $s_n^0 = 41$ S were taken as the initial estimates of these parameters.

The procedure was then used to estimate values for K_2 ($= K_2^{app}$), K_n, g_n, and s_n^0 from weight-average sedimentation velocity data. In practice, the stoichiometry of polymer formation, n, was preset at a constant value for each calculation, and the progressive series of eq 3 and 5 was determined at some value $i = j$ ($j < n$) independent of the last step for polymer formation. This truncation was deemed suitable when the fitted parameters became insensitive to the inclusion of any additional ith step, $j < i < n$, within the linear indefinite association model. A further simplification was made by taking advantage of the insensitivity of eq 9 to changes in certain parameters within different ranges of protein concentration. For example, the values for s_n^0, g_n, and K_n do not affect the calculation in the low concentration range, where the weight fraction of polymer is insignificant, as determined by the equilibrium relation implicit in eq 8.

Typical results of the calculations for relevant combinations of parameters are presented in Table I for two magnesium concentrations. The calculated $\bar{s}$ vs. C curves are compared with the experimental points in Figure 5, where it is seen that the best agreement between the observed and calculated values is given by the model in which the self-association of tubulin proceeds by the formation of a progressive series of aggregates, which is terminated by the formation of a polymer with a stoichiometry of $n = 26$ (mol wt = 2.86×10^6), all species being in rapid equilibrium with monomer (110,000 molecular weight). The best value found for $s_{20,w}^0$ of the polymer is 42 S. The best values obtained for K_2 are 0.224 and 0.332 ml/mg in the presence of 0.008 and 0.016 M $MgCl_2$, respectively.

The species distribution in the self-association reaction in the presence of 0.008 M $MgCl_2$ is shown in Figure 6. At total protein concentrations below about 9 mg/ml, no significant amount of polymer is formed and the description of the self-association in terms of the linear indefinite model of eq 3 is valid. The relative amounts of intermediate aggregates present also decrease with increasing degree of association, so that, in practice, omission of species higher than a hexamer did not introduce any significant error.

It must be emphasized that in the present analysis, the actual magnitudes of the equilibrium constants are dependent upon the values selected for the parameters s_i^0, and g_i, and only the simplest, isodesmic form of progressive self-association has been considered.

Simulation of Sedimentation Velocity Patterns. Recently, Gilbert and Gilbert (1973) have demonstrated that a hypothetical model describing a self-association equilibrium can be supported with considerable success by a precise comparison between theoretical sedimentation patterns and experimental velocity profiles. Therefore, sedimentation velocity profiles have been calculated by using a computer program adopting the method of calculation developed by Cox (1967, 1969, 1971).

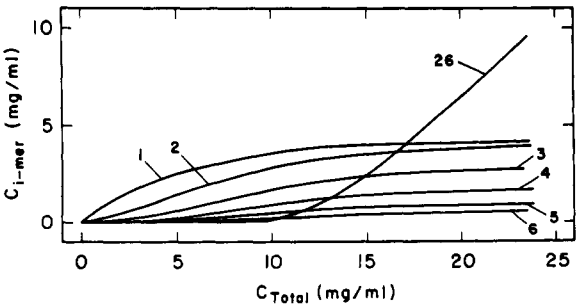

FIGURE 6: Variations in the concentrations of individual species in the self-association of tubulin as a function of the total protein concentration in the presence of 0.008 M $MgCl_2$. The lines are calculated by using the parameters in Table I, set I-1. The numbers indicate the degree of polymerization of each associated species.

Since the sedimentation of a self-associating system in rapid chemical equilibrium is equivalent to the sedimentation of a single concentration-dependent solute (Fujita, 1962), the simulation procedure readily describes the velocity sedimentation of an arbitrary self-associating system in rapid equilibrium in terms of the weight-average sedimentation coefficient. Diffusion can be determined similarly by means of a concentration-dependent average (Steiner, 1954; Cox, 1969). The values of the diffusion coefficients of the i associating species were estimated from the Svedberg equation, using the S_i^0 values of eq 11 and $\bar{v} = 0.736$. The simulation calculation was carried out by predetermining the hydrodynamic coefficients and the appropriate equilibrium constants for the self-association model to be examined. The numerical procedure of Cox (1967, 1969, 1971) was then applied to an initial gradient of protein concentration in a compartmentalized hypothetical sector-shaped centrifuge cell. The output of the calculation was obtained as the profile of the concentration gradient as a function of radial position for a predetermined set of sedimentation times.

Using the data of set I-1 of Table I, a simulated velocity pattern was calculated, and the calculated sedimentation profiles for a series of protein concentrations are shown in Figure 7a. The qualitative agreement with the experimental patterns shown in Figure 3 is striking. In the calculated patterns at the lower concentrations, the single peak is skewed forward and its size and velocity increase progressively with increasing concentration, suggesting a linear indefinite type of progressive association (Holloway and Cox, 1974). At higher concentrations, the profile becomes bimodal and the area under the curve increases exactly as predicted by Gilbert (1955, 1959) for a monomer $\rightleftharpoons$ n-mer equilibrium reaction, $n \geq 3$. The model presented in this work blends these two modes of equilibrium self-association, and the simulated profiles in Figure 7a indicate that complex behavior is expected but that the characteristic features of both types of equilibrium are preserved.

A Direct Comparison of Experimental and Calculated Curves (Gilbert and Gilbert, 1973). Since the method of simulation cannot take into account the effects of restricted diffusion and sedimentation at the meniscus, particularly during rotor acceleration, Gilbert and Gilbert (1973) proposed that an actual experimental velocity profile, presented as concentration vs. radial position be used as initial data. The output of calculated sedimentation at some later time is then compared to the experimental data for an

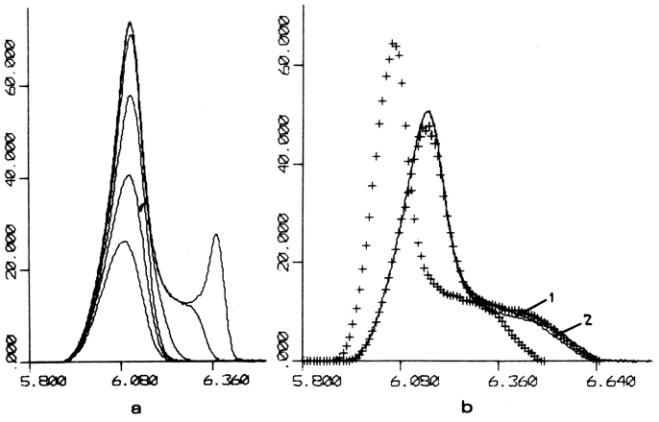

FIGURE 7: Simulated sedimentation velocity profiles of tubulin in a sector-shaped cell at 48,000 rpm. (a) Self-associating conditions of Table I, set I-1. The sedimentation time was 1880 sec. A sharp initial boundary was set at 5.884 cm. The ordinate is the concentration gradient calibrated in units of mg per ml per cm and the abscissa indicates radial position in cm from the center of rotation. The protein concentrations corresponding to the shown patterns are: 4.0, 6.0, 8.0, 10.0, 12.0, and 14.0 mg/ml. (b) The calculated curves (—) correspond to sets: 1, I-1; 2, I-4 of Table I. The experimental concentration gradient profile (+), shown at an early sedimentation time of 1260 sec, was used as the initial boundary data. The theoretical profiles were then calculated for an additional sedimentation time of 720 sec and the curves are shown compared with an experimental profile (+) at 1980 sec. The experimental data are taken from Figure 3, curve 6.

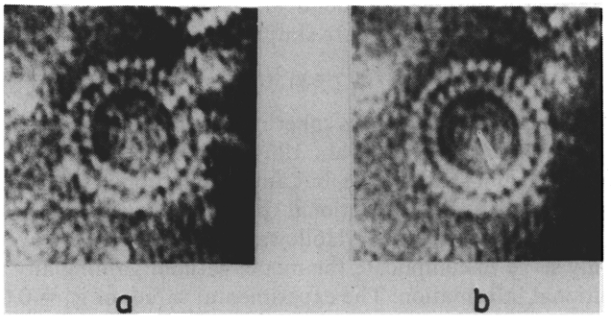

FIGURE 8: Electron micrographs of tubulin negatively stained with uranyl acetate. Image A is a direct view; image B, has been rotated about its center of symmetry by 13.8°, followed by double exposure (see text for details). The primary magnification was ×102,000.

equivalent time. Figure 7b shows the results of such calculations for the data of Table I. The two curves shown are sets I-1 and I-4. Neither curve corresponds exactly to experiment, but the overall agreement between the experimental and calculated patterns again points to the validity of the general features of the proposed model of self-association, although no conclusion can be reached about the exact details of this reaction.

The above analysis in terms of the chosen simple model assumes that no effects such as heterogeneity, time-dependent changes of the properties of the protein, and pressure dependence of equilibrium constants contribute to the interpretation. They may all, however, contribute to the observed sedimentation behavior, although their contributions do not appear to be major.

An Electron Microscopic View of Associated Tubulin. In order to gain further insight into the nature of the end product of the self-association, samples of calf brain tubulin under associating conditions, in PG buffer (pH 7) with 0.016 *M* $MgCl_2$, 20°, were examined by electron microscopy. The pictures obtained (Frigon et al., 1974) clearly reveal the presence of very prominent ring-like structures. These large rings were the only protein aggregates seen with a distinct geometrical configuration; no filamentous or rod-shaped structures were ever seen under these experimental conditions. The overall appearance is that of two closed concentric "beaded" rings. Several distorted views of the structure were apparent, suggesting ring-opening, folding, or partial unraveling. The outside diameter of the double rings was found to be very uniform from image to image and to be 47 ± 3 nm. The inner diameter and the diameter of the circle of contact between the concentric rings were 27 ± 3 and 36 ± 3 nm, respectively. The rings appear to be composed of subunits and the average center-to-center distance between adjacent units is 4.1 ± 0.3 nm.

An estimate of the number of structural subunits around the circle was obtained by rotating the image through various angles about an axis through the center of the ring (Markham et al., 1963). Figure 8a gives a direct view of the ring. Figure 8b is a double exposure of the image in Figure 8a, made after rotating the ring through 13.8°, or 1/26 of the circumferential arc. The subunit structure is clearly enhanced. Rotation through other angles did not lead to any enhancement. The value of 26 coincides with the apparent stoichiometry for the solution polymer, 26 ± 4, although no claim can be made that the number of subunits around the ring is exactly 26. This analysis does not establish the orientation of the 5.8S tubulin dimers in the ring, whether radially or along the perimeter. Furthermore, the possibility has not been excluded that the ring is a double layer of the seen structure.

Hydrodynamic Analysis. The axial ratios of the 5.8S monomer and the 42S polymer were examined by means of the frictional coefficient ratio, f/f_0, which was calculated from

$$\frac{f}{f_0} = \frac{M(1-\bar{v}\rho)}{s_{20,w}{}^0\eta[162\pi^2N^2M(\bar{v}+\delta_1 v_1)]^{1/3}} \qquad (12)$$

where η is the solvent viscosity, M is molecular weight of the sedimenting kinetic unit, N is Avogadro's number, $\bar{v}$ is the protein partial specific volume, 0.736 for tubulin (Lee and Timasheff, 1974), ρ is solvent density, v_1 is the specific volume of solvent, set equal to $\rho_{H_2O}{}^{-1}$, and δ_1 is the amount of water associated with the protein in $g_{H_2O}/g_{protein}$ (Edsall, 1953). For δ_1, the value estimated according to the method of Kuntz (1971) was selected (Lee and Timasheff, 1974). Allowing for the nonaccessibility to solvent of internal amino acid residues, a reasonable value of δ_1 for tubulin is 0.36 g/g. With these values, for the 5.8S tubulin species, f/f_0 = 1.24, which corresponds to an axial ratio, a/b, of 3.9 for a prolate ellipsoid of revolution and 4.2 for an oblate ellipsoid (Svedberg and Pedersen, 1940). The corresponding Stokes radius, R_0 (Tanford, 1963), is 4.4 nm. A similar calculation for the 42S polymer with a molecular weight of 2.86×10^6 gives a value of f/f_0 = 1.47 and axial ratios of 8.4 for a prolate and 10.4 for an oblate ellipsoid of revolution. The last value corresponds to an ellipsoid with proportions similar to those estimated for the ring observed in the electron microscope.

The relation between the protein complex seen in the electron microscope and the tubulin polymer formed in solution was tested by calculating its expected sedimentation coefficient by using the method of Kirkwood (1954). For this purpose, the ring structure was simplified to a plane polygon with subunits of the complex lying at its vertices.

According to the Kirkwood (1954) theory, if the complex is composed of an arbitrary array of connected identical subunits, which may be fluctuating or fixed relative to one another, it is possible to calculate its sedimentation coefficient by

$$s = \frac{M(1-\bar{v}\rho)}{nN}\left(\frac{1}{f}+\frac{1}{6\pi\eta n}\sum_{l=1}^{n}\sum_{\substack{s=1\\ l\neq s}}\langle R_{ls}\rangle^{-1}\right) \quad (13)$$

where f is the frictional coefficient of the subunit, n is the number of subunits in the array, and $\langle R_{ls}\rangle$ is the time-averaged distance between the l and s subunits. In the proposed structure of the plane polygon, R_{ls} is the distance between the l and s vertices. It can be readily calculated by a recursion formula in the form of:

$$R_{ls} = \frac{a|\sin[\theta/2(s-1)]|}{\sin[\theta/2]} \quad (14)$$

where a is the length of a side of an n-sided regular polygon and $\theta = 2\pi/n$.

In the present calculation, f was taken as the frictional coefficient of either the tubulin dimer or the tubulin tetramer. The dimension a was calculated according to a selected radial distance to a vertex of the polygon taken as the value of the radius from the center of the double ring observed in the electron microscope to a point on the circle of contact between the concentric rings. Sedimentation coefficients, calculated for a variety of parameters, are shown in Table II. The results indicate that a plane polygonal arrangement of either 26 ± 4 subunits, each with molecular weight 110,000 and frictional coefficient $f = 8.3 \times 10^{-8}$, or 13 ± 2 subunits, each with molecular weight 220,000 and frictional coefficient $f = 9.3 \times 10^{-8}$–12.5×10^{-8}, located about the circumference of the polygon at 18 ± 2 nm from the center, describes satisfactorily the sedimentation behavior of the polymer. The calculated polymer sedimentation coefficient is 43 ± 3 S; the observed sedimentation coefficient is 42 ± 2 S. It appears, therefore, that the closed double-ring protein complex observed by electron microscopy describes well the structure of the polymer detected by sedimentation velocity when calf brain tubulin is induced to self-associate by the addition of magnesium ions to the system and may indeed be a true picture of the structure in solution.

Concluding Remarks. The presently described self-association of tubulin is mediated by the presence of a ligand, Mg^{2+} ions. Cann and Goad (1972) have shown that ligand-mediated self-association reactions may give rise to complicated sedimentation behavior. Such behavior has been demonstrated for several systems, e.g., the Ca^{2+}-induced dimerization of hemocyanin (Morimoto and Kegeles, 1971) and, in fact, the vinblastine-induced self-association of tubulin (Weisenberg and Timasheff, 1970; Lee and Timasheff, 1975). The conditions for such behavior generally require that a sufficiently strong interaction of ligand with protein take place at a ligand concentration sufficiently low to establish stable concentration gradients of ligand across the sedimenting boundary in the centrifuge cell (Cann, 1970). The conditions for the self-association of tubulin in the presence of Mg^{2+} do not meet these requirements, since the large excess of Mg^{2+} over protein, required for the reaction, precludes the formation of stable Mg^{2+} concentration gradients.

By treating the sedimentation velocity data for tubulin in the presence of Mg^{2+} solely in terms of the self-association of the protein, a self-consistent equilibrium analysis has been made. In the range of Mg^{2+} concentrations from 0.001 to 0.005 *M*, tubulin self-associates in a progressive manner and the degree of association is increased by increasing the protein concentration up to the highest protein concentration accessible in these studies. At higher Mg^{2+} concentrations, 0.008–0.016 *M*, tubulin polymerization proceeds to the formation of a rapidly sedimenting component which is in rapid equilibrium with the tubulin dimer although a significant amount of progressive self-association is always observed. These two aspects of the self-association cannot be treated as alternative modes of reaction, but must be considered as contributing to the same self-association process. The end product of this self-association can be described best by a polymer, composed of approximately 26 dimers, having the geometry of a closed-ring structure.

Table II: Polymer Sedimentation Coefficients Calculated by the Kirkwood Theory.

Molecular Weight ($\times 10^{-6}$)	No. of Subunits	Subunit Frictional Coefficient ($\times 10^{8}$)	Radius of Particle (nm)	S ($\times 10^{13}$)
2.86	26	8.3	18	45
2.86	26	8.3	19	43
2.86	26	8.3	16	50
2.86	26	8.3	14	58
2.86	26	8.3	24	36
2.0	18	8.3	18	31
3.6	33	8.3	18	59
2.86	13	9.3	18	42
2.86	13	10.4	18	41
2.86	13	12.5	18	39
5.72	26	10.4	18	89

At present, any morphological connection between the ring polymer formed by the self-association of tubulin and the mechanism of assembly of microtubules is open to question. It has been reported (Borisy and Olmsted, 1972; Shelanski et al., 1973) that a particulate fraction of brain cell homogenates is required for microtubule assembly in vitro. Disc-like structures, seen in the electron micrographs of this particulate fraction, have been proposed as the nucleation centers for the growth of microtubules (Borisy and Olmsted, 1972). The dimensions reported for these discs, however, are highly different from those of the rings described in this paper. More recently, Kirschner et al. (1974) have reported electron microscopic evidence that depolymerization by chilling of microtubules gives rise to spiral-shaped and double-ringed structures similar to the closed-ring polymer described in this paper. These authors have assigned to these structures the role of intermediates in the formation of microtubules; specifically, they state that microtubule growth occurs through a structural transition of rings to spirals, which unravel after adding on to the ends of existing microtubules, elongating in this manner the existing tubular structures. While the published electron micrographs of these structures appear to be markedly similar to the double-ring polymers described in this paper (Frigon et al., 1974), closer analysis indicates that the structures must not be identical. Kirschner and Williams (1974) report that the double rings which they have observed are composed of an outer circle containing 24 subunits of molecular weight 55,000 and an inner circle containing 18 such subunits, which gives an overall molecular weight of 2.3×10^6. Furthermore, their analysis (Weingarten et al., 1974) of this

double ring in terms of the Kirkwood hydrodynamic theory gave a sedimentation coefficient of 36 S, which is in agreement with the experimental value which they have reported for this structure (Kirschner and Williams, 1974). They also state that these rings are not in equilibrium with the 5.8S monomer (Weingarten et al., 1974), but that the 5.8S monomers and the subunits which form the rings are chemically different from each other.

From the above discussion, it is evident that morphologically similar assemblies of tubulin can be formed either by the depolymerization of microtubules or as the end product of the Mg^{2+}-induced self-association of purified tubulin. However, the role of such structures, if any, in the dynamic equilibrium of microtubule formation cannot be established on the basis of the evidence available at present. Indeed, up to the present, there have been no reports of any equilibrium distribution of rings in vivo.

Acknowledgments

The authors would like to thank Dr. James C. Lee for many valuable discussions and suggestions in the course of these studies and Dr. Manuel S. Valenzuela for his assistance with the electron microscopic work.

References

Borisy, G., and Olmsted, J. (1972), *Science 177,* 1196–1197.

Cann, J. R. (1970), Interacting Macromolecules: Theory and Practice of Their Electrophoresis, Ultracentrifugation and Chromatography, New York, N.Y., Academic Press.

Cann, J. R., and Goad, W. B. (1972), *Arch. Biochem. Biophys. 153,* 603–609.

Chun, P. W., and Kim, S. J. (1969), *Biochemistry 8,* 1633–1643.

Chun, P. W., Kim, S. J., Stanley, C. A., and Ackers, G. K. (1969), *Biochemistry 8,* 1625–1632.

Cox, D. J. (1967), *Arch. Biochem. Biophys. 119,* 230–239.

Cox, D. J. (1969), *Arch. Biochem. Biophys. 129,* 106–123.

Cox, D. J. (1971), *Arch. Biochem. Biophys. 142,* 514–526.

Edsall, J. T. (1953), in The Proteins, Vol. 1B, Neurath, H., and Bailey, K., Ed., New York, N.Y., Academic Press, pp 549–726.

Frigon, R. P., and Lee, J. C. (1972), *Arch. Biochem. Biophys. 153,* 587–589.

Frigon, R. P., Valenzuela, M. S., and Timasheff, S. N. (1974), *Arch. Biochem. Biophys. 165,* 442–443.

Fujita, H. (1962), Mathematical Theory of Sedimentation Analysis, New York, N.Y., Academic Press.

Gilbert, G. A. (1955), *Discuss. Faraday Soc. No. 20,* 68–71.

Gilbert, G. A. (1959), *Proc. R. Soc. London, Ser. A, 250,* 377–388.

Gilbert, G. A. (1963), *Proc. R. Soc. London, Ser. A, 276,* 354–366.

Gilbert, L. M., and Gilbert, G. A. (1973), *Methods Enzymol. 27,* 273–296.

Goldberg, R. J. (1953), *J. Phys. Chem. 57,* 194–202.

Holloway, R. R., and Cox, D. J. (1974), *Arch. Biochem. Biophys. 160,* 595–602.

Josephs, R., and Harrington, W. F. (1968), *Biochemistry 7,* 2834–2847.

Kirkwood, J. G. (1954), *J. Polym. Sci. 12,* 1–14.

Kirschner, M. W., and Williams, R. C. (1974), *J. Supramol. Struct. 2,* 412–428.

Kirschner, M. W., Williams, R. C., Weingarten, M., and Gerhart, J. C. (1974), *Proc. Natl. Acad. Sci. U.S.A. 71,* 1159–1163.

Kuntz, I. D. (1971), *J. Am. Chem. Soc. 93,* 514–516.

Lee, J. C., Frigon, R. P., and Timasheff, S. N. (1973), *J. Biol. Chem. 248,* 7253–7262.

Lee, J. C., and Timasheff, S. N. (1974), *Biochemistry 13,* 257–265.

Lee, J. C., and Timasheff, S. N. (1975), *J. Biol. Chem.* (in press).

Magar, M. E. (1973), Data Analysis in Molecular Biology, New York, N.Y., Academic Press.

Markham, R. M., Frey, S., and Hills, G. J. (1963), *Virology 20,* 88–102.

Morimoto, K., and Kegeles, G. (1971), *Arch. Biochem. Biophys. 142,* 247–257.

Nichol, L. W., Bethune, J. L., Kegeles, G., and Hess, E. L. (1964), in The Proteins, 2nd ed, Vol. 2, Neurath, H., Ed., New York, N.Y., Academic Press, pp 305–403.

Olmsted, J. B., and Borisy, G. G. (1973), *Annu. Rev. Biochem. 42,* 507–540.

Reisler, E., Pouyet, J., and Eisenberg, H. (1970), *Biochemistry 9,* 3095–3102.

Richards, E. G., Teller, D. C., Hoagland, V. O., Jr., Haschemeyer, R. H., and Schachman, H. K. (1971), *Anal. Biochem. 41,* 215–247.

Schachman, H. K. (1959), Ultracentrifugation in Biochemistry, New York, N.Y., Academic Press.

Shelanski, M. L., Gaskin, F., and Cantor, C. (1973), *Proc. Natl. Acad. Sci. U.S.A. 70,* 765–768.

Steiner, R. F. (1954), *Arch. Biochem. Biophys. 49,* 400–416.

Svedberg, T., and Pedersen, K. O. (1940), The Ultracentrifuge, Oxford, England, Clarendon Press.

Tanford, C. (1963), Physical Chemistry of Macromolecules, New York, N.Y., Wiley.

Townend, R., Winterbottom, R. J., and Timasheff, S. N. (1960), *J. Am. Chem. Soc. 82,* 3161–3168.

Weingarten, M. D., Suter, M. M., Littman, D. R., and Kirschner, M. W. (1974), *Biochemistry 13,* 5529–5537.

Weisenberg, R., Borisy, G., and Taylor, E. (1968), *Biochemistry 7,* 4466–4479.

Weisenberg, R. C., and Timasheff, S. N. (1970), *Biochemistry 9,* 4110–4116.

Weisenberg, R. (1972), *Science 177,* 1104–1105.